

# Analysis of RXTE-PCA Observations of SMC X-1

S.Ç. İnam<sup>1</sup>, A. Baykal<sup>2</sup>, E. Beklen<sup>2,3</sup>

<sup>1</sup> Department of Electrical and Electronics Engineering,  
Başkent University, 06530 Ankara, Turkey  
inam@baskent.edu.tr

<sup>2</sup> Physics Department,  
Middle East Technical University, 06531 Ankara, Turkey  
elif@astroa.physics.metu.edu.tr

<sup>3</sup> Physics Department, Süleyman Demirel University, 32260 Isparta, Turkey

## Abstract

We present timing and spectral analysis of RXTE-PCA observations of SMC X-1 between January 1996 and December 2003. Using our timing analysis and the previous studies, we construct a  $\sim 30$  year long pulse period history of the source. We show that frequency derivative shows long (i.e. more than a few years) and short (i.e. order of days) term fluctuations. We revise timing solution of the source and resolve the eccentricity as 0.00089(6). We also find an orbital decay rate of  $\dot{P}_{orb}/P_{orb} = -3.402(7) \times 10^{-6} \text{ yr}^{-1}$  which is close to the previous results. From the spectral analysis, all spectral parameters except Hydrogen column density show no significant variation with time and X-ray flux. Hydrogen column density is found to be higher as X-ray flux gets lower. This may be due to the increase in soft absorption when the pulsar is partially obscured as in Her X-1 or may just be an artifact of the tail of a soft excess in energy spectrum.

**Keywords:** X-rays: binaries, pulsars, individual: SMC X-1 , stars: neutron, accretion, accretion discs

## 1 Introduction

The high mass X-ray binary (HMXB) system SMCX-1/Sk 160 consists of a neutron star with a mass of  $\sim 1.06M_{\odot}$  (van der Meer et al. 2007) and a spin period of 0.71s (Lucke et al.1976), accreting from the B0I star Sk 160 with a mass of  $\sim 17.2M_{\odot}$  (Reynolds et al. 1993). Orbital period of the system is  $\sim 3.9$  days (Schreier et al. 1972). The system has been observed with several observatories since it was discovered during a rocket flight (Price et al. 1971). It is the only discovered HMXB with a supergiant companion in SMC so far (Galache et al. 2008).

From the pulse timing studies, the source was observed to be spinning up since it was discovered (Wojdowski et al. 1998). Levine et al. (1993) and Wojdowski et al (1998) found an orbital period decay in the system with  $P_{orb}/\dot{P}_{orb}$  of  $\sim 3.4 \times 10^{-6} \text{ yr}^{-1}$ .

SMC X-1 also exhibits super-orbital X-ray flux variations like the 35 day cycle of Her X-1 (Gruber& Rothschild, 1984). Average super-orbital period of the source is  $\sim 55$  days (Wojdowski et al.1998; Trowbridge et al.2007). The super-orbital X-ray flux variations of SMC X-1 are thought to be due to the precession of a warped accretion disk (Wojdowski et al.1998).

In this paper, we present timing and spectral analysis of RXTE (Rossi X-ray Timing Explorer) observations of SMC X-1 between January 1996 and December 2003. In the next section, we give brief information about instruments and observations. In Section 3, we present the results of timing analysis, including pulse period history and timing solution of the source. In Section 4, X-ray spectral analysis of the source is presented.

## 2 Instruments and Observations

We analyzed data from Proportional Counter Array (PCA) onboard RXTE (Jahoda et al 1996) of SMC X-1 between January 1996 and December 2003 (MJD 50093-52988).

The RXTE-PCA consists of an array of 5 Proportional Counters (PCU) operating in the 2-60 keV energy range, with a total effective area of approximately  $7000 \text{ cm}^2$  and a field of view of  $\sim 1^\circ$  FWHM. Data obtained from top xenon layers of PCUs were used for better statistics. For the observations after May 2000, for which the propane layer for PCU0 was lost, data obtained from PCU0 was not used in the spectral analysis.

Excluding X-ray eclipses, we used data obtained from  $\sim 130$  pointings with a total exposure of  $\sim 250$  ksec for the timing analysis. During the observations between 1998 October 16 and 1998 November 24, with an exposure of  $\sim 23$  ks, the data were contaminated due to the outburst of the nearby transient X-ray pulsar XTEJ0111.2-7317 (Chakrabarty et al 1998). We did not use these observations in the X-ray spectral analysis.

## 3 Timing Analysis

For the timing analysis, all lightcurves were generated using Good Xenon data and were background corrected using background estimator models. We binned the resulting lightcurves into 0.035s bins for timing analysis and corrected them to the barycenter of the Solar system. A template pulse profile from each RXTE observation was constructed by folding the data on the period which had the greatest power in the periodogram. Pulse arrival times were found by cross-correlating the pulse profiles obtained from  $\sim 200$ s long segments with the template pulse profile. Both the template and cross-correlated pulse profiles consisted of 20 phase bins. Crosscorrelation was performed by using the harmonic representation of pulse profiles (Deeter & Boynton 1985). In order to obtain pulse arrival times, the pulse profiles were expressed in terms of harmonic series and cross-correlated with the template pulse profile. Initially, we found pulse arrival times obtained from a series of observations with a time span of  $\sim 6$  days around MJD 50324.7. These pulse arrival times can be fitted to an expression to obtain timing solution (Deeter, Boynton, & Pravdo 1981). We firstly assumed a circular orbit ( $e=0$ ) and therefore this expression became

$$\delta t = \frac{\delta P}{P}(t - t_0) + \frac{1}{2} \frac{\dot{P}}{P}(t - t_0)^2 + x \sin(l). \quad (1)$$

Table 1: Timing Solution of SMC X-1

parameters	Model (This Work)
Timing Epoch (MJD)	50326.62356961(9)
$\nu$ (Hz)	1.413630801(4)
$\dot{\nu}$ ( $10^{-11}$ Hz.s $^{-1}$ )	3.279(5)
Orbital Period (days)	3.89220909(4)
$a/c \sin I$ (lt-s)	53.4876(9)
Orbital Epoch	MJD 50324.691861(8)
$\dot{P}_{orbit}/P_{orbit}$ ( $10^{-6}$ yr $^{-1}$ )	-3.402(7)
Eccentricity	0.00089(6)
w (longitude of periastron)	166(12)

Here  $t_0$  is the mid-time of the observation;  $\delta P$  is the deviation from mean pulse period;  $\dot{P}$  is the time derivative of the pulse period;  $x = a/c \sin(i)$  is the light traveltime for projected semimajor axis (where  $i$  is the inclination angle between the line of sight and the orbital angular momentum vector);  $l = 2\pi(t - T_{\pi/2})/P_{orbit} + \pi/2$  is the mean orbital longitude at  $t$ ;  $T_{\pi/2}$  is the epoch when the mean orbital longitude is equal to  $90^\circ$ ;  $P_{orbit}$  is the orbital period of the system. In order to improve the fit, we used the whole expression containing terms corresponding to an eccentric orbit as

$$\delta t = \frac{\delta P}{P}(t-t_0) + \frac{1}{2} \frac{\dot{P}}{P}(t-t_0)^2 + x \sin(l) - \frac{3}{2} x e \sin(w) + \frac{1}{2} x e \cos(w) \sin(2l) - \frac{1}{2} x e \sin(w) \cos(2l). \quad (2)$$

In Equation 2,  $e$  is the eccentricity and  $w$  is the longitude of periastron. The periodic trend of the pulse arrival times yields an eccentric orbit ( $e=0.00089(6)$ ) with an orbital period of 3.89220909(4) days (numbers in paranthesis denote  $1\sigma$  uncertainties in the least significant figures hereafter). Table 1 presents the timing solution of SMC X-1. Figure 1 presents the pulse arrival times after the removal of the quadratic trend (or intrinsic  $-\dot{P}$ ) together with the residuals of circular ( $e=0$ ) and eccentric orbit models respectively.

In Table 2, we present the orbital epoch ( $T_{\pi/2}$ ) measurements from different observatories and orbital cycle number ( $N$ ). In Figure 2, we present observed minus calculated values of orbital epochs ( $T_{\pi/2} - n < P_{orbit} > - < T_{\pi/2} - n < P_{orbit} >>$ ) relative to the constant orbital period ( $< P_{orbit} > = 3.892188$  days). It should be noted that the rightmost point indicated as "RXTE Point" is our result and other points were already published before (see Figure 7 in Wojdowski et al. 1998). A quadratic fit to the epochs from all experiments yielded an estimate of the rate of period change  $\dot{P}_{orb}/P_{orb} = -3.402(7) \times 10^{-6}$  yr $^{-1}$ .

For the other observations between MJD 50093 and MJD 52988 (each having  $\sim 1-2$  ksec exposure), we calculated pulse periods from the slopes of arrival times. These periods were orbitally corrected using the orbital parameters listed in Table 1. We present whole pulse period history of the source in Table 3 and Figure 3 including our results. From Figure 3, it is evident that the source spins up continuously between MJD  $\sim 40000$  and MJD  $\sim 53000$  with a varying spin-up rate. In Table 4, average spin-up rate values of the source are listed.

Table 2: Orbital Epoch Measurements of SMC X-1

$T_{\pi/2}$ (MJD)	N	Observatory	Reference
40963.99(2)	-481	Uhuru	1,2
42275.65(4)	-144	Copernicus	1,3
42836.1828(2)	0	SAS 3	1,4
42999.6567(16)	42	Ariel V	1,5
43116.4448(22)	72	Cos B	1,6
46942.47237(15)	1055	Ginga	1,7
47401.744476(7)	1173	Ginga	1,7
47740.35906(3)	1260	Ginga	1,7
48534.34786(35)	1464	ROSAT	1
49102.59109(82)	1610	ASCA	1
49137.61911(50)	1619	ROSAT	1
50091.170(63)	1864	RXTE	1
50324.691861(8)	1924	RXTE	8

References: (1) Wojdowski et al. 1998; (2) Schreier et al. 1972; (3) Tuohy & Rapley 1975; (4) Primini et al. 1977; (5) Davison 1977; (6) Bonnet-Bidaud et al. 1981; (7) Levine et al. 1993; (8) This work

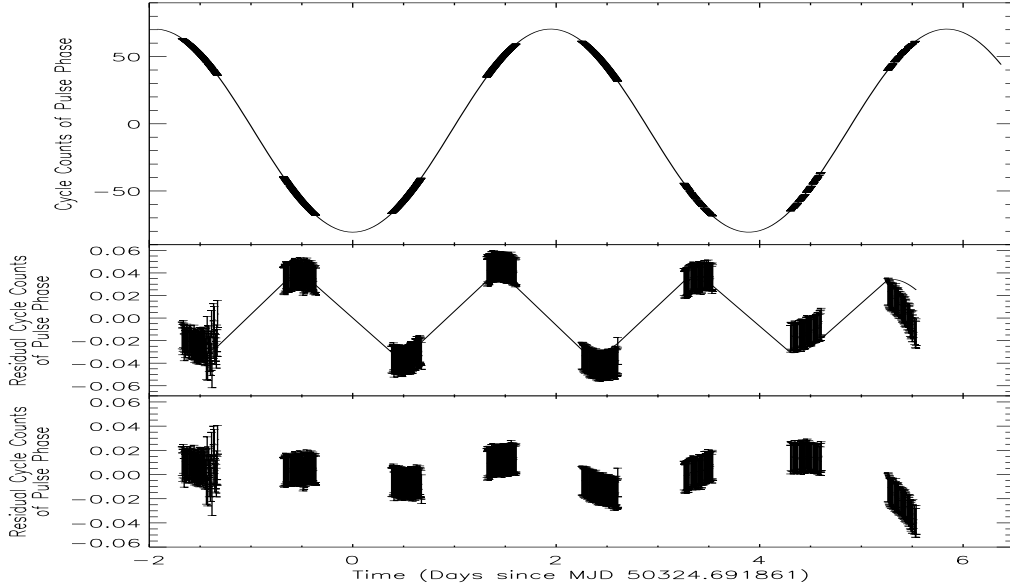


Figure 1 – Arrival times (top panel), and residuals after fitting arrival times to a circular (middle panel) and elliptical orbital model (lower panel).

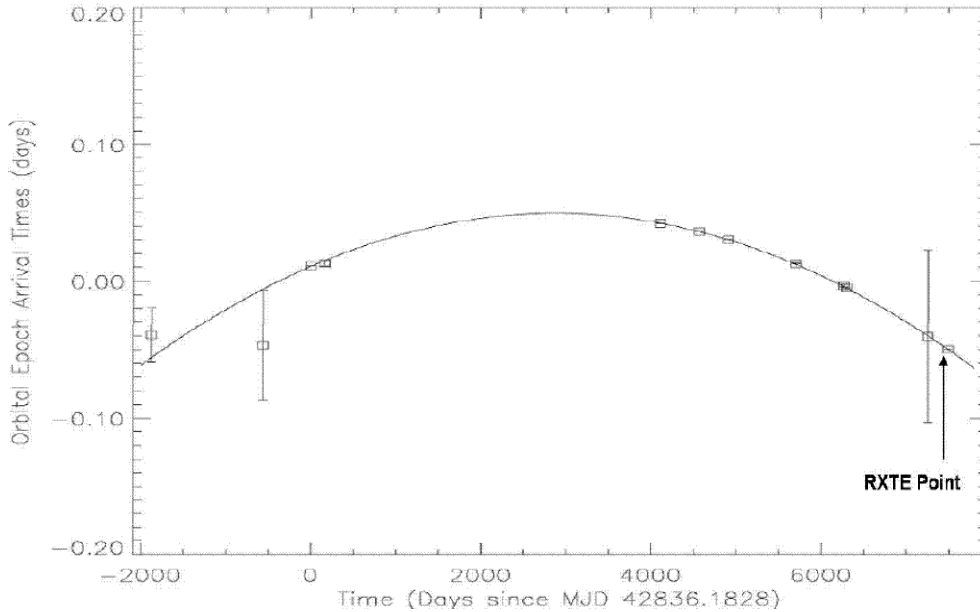


Figure 2 – Orbital Epoch Arrival Times of SMC X-1. From the quadratic fit to the data, an orbital period decay with  $P_{orbit}/P_{orbit} = -3.402(7) \times 10^{-6} \text{ yr}^{-1}$  is found.

## 4 Spectral Analysis

Standard-2 data of each RXTE observation used in timing analysis were used in spectral analysis except those between 1998 October 16 and 1998 November 24 which were contaminated due to the outburst of the nearby transient X-ray pulsar XTEJ0111.2-7317 (Chakrabarty et al 1998). Spectrum, background and response matrix files were created using FTOOLS 6.3 data analysis software. We used background subtracted spectra in our analysis. Energy channels corresponding to the 3-25 keV energy range were used to fit the spectra. We ignored photon energies lower than 3 keV and higher than 25 keV and 1% systematic error was added to the errors.

To fit the spectra, we used a power law model with an high energy cutoff and a Gaussian component peaking at 6.7 keV (Angelini et al 1991). We also tried to add a partial covering absorption component (Nielsen et al 2004), but adding this model component did not improve the fit.

Table 4 shows best fit parameters of the spectral model for two sample observations. In general, we found no significant variation of power law index, high energy cut-off and e-fold energy with time, orbital phase and X-ray flux. We found that Hydrogen column density gets higher when X-ray flux is lower (see Figure 4).

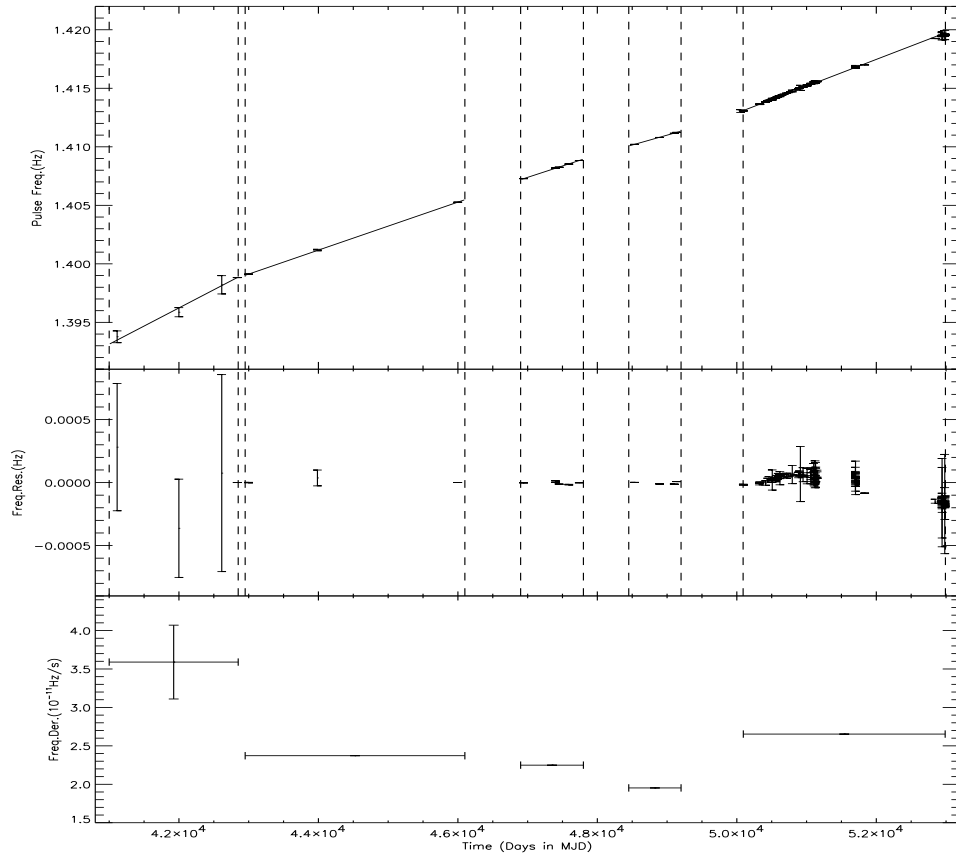


Figure 3 – **(top)** and **(middle)** Pulse frequency history and residuals of SMC X-1 after a linear fit obtained from 5 different intervals listed in Table 4. **(bottom)** Frequency derivative history. Dashed lines in top and middle panels and horizontal error bars in the bottom panel indicate time intervals in which linear fits were performed.

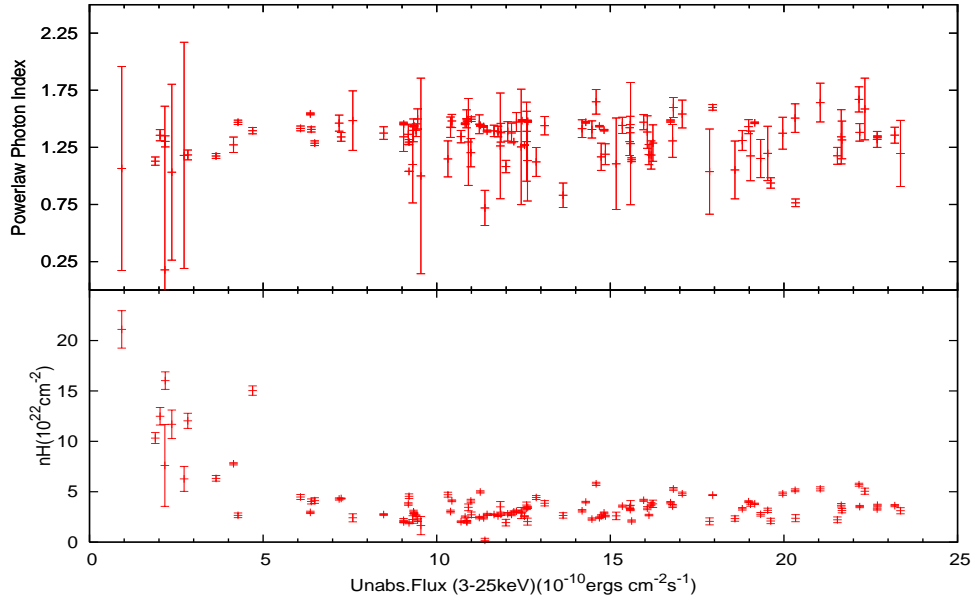


Figure 4 – Dependence of photon index and  $n_H$  on 3-25 keV unabsorbed X-ray flux.

## 5 Conclusion

In this paper, we presented timing and spectral analysis of RXTE-PCA observations of SMC X-1 with a time span of about 8 years. Our timing analysis helped us to construct a  $\sim 30$  year long pulse period history of the source (see Figure 3). From timing analysis, we revised timing solution of the source and resolved an eccentricity value. We also confirmed the orbital decay reported before. From the spectral analysis, we found that all spectral parameters except Hydrogen column density showed no significant variation with time and X-ray flux.

The timing solution of the source revealed that the binary orbit has an eccentricity of 0.00089(6). Wojdowski et al. (1998) had found a circular orbit solution and Levine et al. (1993) had only found an upper limit of 0.00004 for eccentricity. Our present value is more than 20 times greater than the upper limit found by Levine et al. 1993.

From Figure 3, it is seen that SMC X-1 spins up continuously for  $\sim 30$  years. We found that average long term spin-up rate of the source between MJD 50093.048 and MJD 52987.640 (whole time span of our analysis) is  $2.65343816(7) \times 10^{-11}$  Hz s $^{-1}$ .

Spin-up rate of a source with a persistent accretion disk can be expressed as

$$\dot{\nu} \simeq 2.2 \times 10^{-12} \mu_{30}^{2/7} m_x^{-3/7} R_6^{6/7} I_{45}^{-1} L_{37}^{6/7} \text{ Hz s}^{-1}, \quad (3)$$

where  $\dot{\nu}$  is first time derivative of the spin frequency,  $\mu_{30}$  is the magnetic moment of the neutron star in units of  $10^{30}$  Gauss cm $^3$ ,  $m_x$  is the mass of the neutron star in units of solar mass,  $R_6$  is the radius of the neutron star in units of cm,  $I_{45}$  is the moment of inertia of the

neutron star in terms of  $10^{45}$  g cm<sup>2</sup>, and  $L_{37}$  is the luminosity of the neutron star in units of  $10^{37}$  erg s<sup>-1</sup> (Ghosh& Lamb, 1979). Using a distance value of 61kpc (Keller& Wood 2006) and a flux of  $1.2 \times 10^{-9}$  ergs cm<sup>-2</sup> s<sup>-1</sup> (see Figure 5), luminosity of SMC X-1 is  $\sim 5.5 \times 10^{38}$  erg s<sup>-1</sup>. Assuming magnetic moment of  $10^{30}$  Gauss cm<sup>3</sup>, mass of  $1.4M_{\odot}$ , radius of  $10^6$  cm, moment of inertia of  $10^{45}$  g cm<sup>2</sup>, we find  $\dot{\nu}$  to be  $\sim 5.9 \times 10^{-11}$  Hz s<sup>-1</sup>. This value is of the order of the observed spin-up rate value of the source.

From Figure 3 and Table 4, it is evident that the long term spin-up rate of SMC X-1 varies significantly. From Equation 3, this variation may -in principle- be related to a change in X-ray luminosity of the source. However, previous X-ray observations of the source were performed by different X-ray observatories and/or in different energy bands. Moreover these observations are sparsely distributed and average X-ray flux of these observations are not likely to represent an average X-ray flux for the intervals for which the pulse frequency derivatives were found. Therefore, it is not possible to test whether variation in long term spin-up rate is related to a change in X-ray luminosity or not.

From Table 1, spin-up rate obtained from  $\sim 6$ days long observation around MJD 50324.7 is  $3.279(5) \times 10^{-11}$  Hz s<sup>-1</sup>. This is about 20% greater than the long term spin-up rate between MJD 50093 and 52988. Assuming that the pulse frequency variations can be explained in terms of random walk model in pulse frequency (Ogelman& Baykal 1993), one can express the pulse frequency derivative variations as  $\langle \Delta\dot{\Omega}^{1/2} \rangle = \sqrt{\frac{S}{t}}$  where S is the noise strength and t is the time interval at which the pulse frequency derivatives are observed. Therefore it is natural to observe high pulse frequency derivative fluctuations at shorter time scales.

From timing analysis, we obtained a new orbital epoch of SMC X-1 from RXTE observations. Using this new epoch and previous results (Wojdowski et al. 1998), we found that there is an orbital decay with  $P_{orbit}/\dot{P}_{orbit}$  of  $-3.402(7) \times 10^{-6}$  yr<sup>-1</sup>. This value is similar to the values found by Wojdowski et al. (1998) and Levine et al. (1993).

From the spectral analysis, we found that all of the spectral parameters except Hydrogen column density did not vary significantly. Hydrogen column density was found to be higher as X-ray flux gets lower. Increase in Hydrogen column density with a decrease in X-ray flux is also observed in Her X-1 (Inam& Baykal, 2005) and may be due the fact that soft absorption becomes stronger whenever there is a partial obscuration of the neutron star due to the X-ray eclipses and warping of the accretion disk. The increase in Hydrogen column density may also be an artifact of the simple absorbed power law model. Paul et al. (2002) showed that SMC X-1 has soft excess especially for energies  $\lesssim 3$  keV. Although we used photon energies greater than 3keV in our analysis, tail of a soft spectral component may affect low energies in our analysis and as a result we might have misidentified corresponding changes in energy spectrum as variations in Hydrogen column density parameter.

## 6 Acknowledgements

## 7 References

Angelini L., Stella L. and White N.E., 1991, ApJ, 371, 332

Bonnet-Bidaud J. M., van der Klis M., 1981, A&A, 97, 134



- Chakrabarty D., Levine A. M., Clark G. W., Takeshima T., 1998, IAUC, 7048
- Davison P. J. N., 1977, MNRAS, 179, 15
- Deeter J. E., Boynton P. E., Pravdo S. H., 1981, ApJ, 247, 1003
- Deeter J. E., Boynton P. E., 1985, in Proc. Inuyama Workshop on Timing Studies of X-Ray Sources, ed. S. Hayakawa & F. Nagase (Nagoya: Nagoya Univ.), 29
- Galache J. L., Corbet R. H. D., Coe M. J., Laycock S., Schurch M. P. E., Markwardt C., Marshall F. E., Lochner J., 2008, ApJS, 177, 189
- Gruber D. E., Rothschild R. E., 1984, ApJ, 283, 546
- Inam S. C., Baykal A., 2005, MNRAS, 361, 1393
- Henry P., Schrier E., 1977, ApJ, 212, L13
- Jahoda K., Swank J. H., Giles A. B., Stark M. J., Strohmayer T., Zhang W., Morgan, E. H., 1996, SPIE, 2808, 59
- Kahabka P., Li X.D., 1991, A&A, 345, 117
- Kunz M., Gruber D.E., Kendziorra E. et al. 1993, A&A, 268, 116
- Levine A., Rappaport S., Deeter J.E., Boynton P.E., Nagase F., 1993, ApJ, 410, 328
- Lucke R., Yentis D., Friedman H., Fritz G., Shulman S., 1976, ApJL, 206, 25
- McBride V.A., Coe M.J., Bird A.J., Dean A.J., Hill A.B., McGowan K.E., Schurch M.P.E., Udalski A., Soszynski I., Finger M., Wilson C.A., Corbet R.H.D., Negueruela I., 2007, MNRAS, 382, 743
- Naik S. and Paul B., 2004, A&A, 418, 655
- Neilsen J., Hickox R. C., Vrtilik S. D., 2004, ApJL, 616, 135
- Paul B., Nagase F., Endo T., Dotani T., Yokogawa J., Nishiuchi M., 2002, ApJ, 579, 411
- Price R. E., Groves D. J., Rodrigues R. M., Seward F. D., Swift C. D., Toor A., 1971, ApJL, 168, 7
- Primini F.A., 1977, PhD thesis submitted to Massachusetts Institute of Technology
- Reynolds A. P., Hilditch R. W., Bell S. A., Hill G., 1993, MNRAS, 261, 337

Schreier E., Giacconi R., Gursky H., Kellogg E., Tananbaum H., 1972, ApJL, 178, 71

Trowbridge, S., Nowak M. A., Wilms, J., 2007, ApJ, 670, 624

Tuohy I. R., Rapley, C. G., 1975, ApJL, 198, 69

van der Meer A., Kaper L., van Kerkwijk M. H., Heemskerk M. H. M., van den Heuvel  
E. P. J., 2007, A&A, 473, 523

Vrtilek S.D., Raymond J.C., Boroson B., McCray R. 2005, 626, 307

Wojdowski P., Clark George W., Levine Alan M., 1998, ApJ, 502, 253

Yentis D., Shulman S., Mckee J.D., Rose W.K., 1977, Astrophys. Lett., 19, 53

Table 3: Pulse Frequency History of SMC X-1

Proposal ID or Observatory	MJD (days)	Pulse Period <sup>1</sup>	References
Uhuru	41114.200	1.39377(51)	Henry & Schreier, 1977
Aerobee	41999.600	1.3959(4)	Yentis et al 1977
Apollo-Soyuz	42613.799	1.3982(8)	Henry & Schreier, 1977
SAS 3	42836.183	1.3988247(1)	Wojdowski et al 1998
Ariel V	42999.6567	1.3991225(23)	Wojdowski et al 1998
Einstein	43985.907	1.401180(63)	Wojdowski et al 1998
EXOSAT	45998.500	1.4052680772(8)	Kunz et al 1993
Ginga	46942.4724	1.407277083(71)	Levine et al 1993
HEXE	47399.500	1.4081806(29)	Kunz et al 1993
Ginga	47401.744	1.408171707(30)	Levine et al 1993
HEXE	47451.500	1.4082567(30)	Kunz et al 1993
HEXE	47591.000	1.4085229(30)	Kunz et al 1993
Ginga	47740.3591	1.408827913(64)	Levine et al 1993
ROSAT 1	48534.3479	1.41021063(68)	Wojdowski et al 1998
ROSAT 2	48892.4191	1.4108022(12)	Wojdowski et al 1998
ASCA	49102.5911	1.4111556(18)	Wojdowski et al 1998
ROSAT 3	49137.6191	1.4112350(10)	Wojdowski et al 1998
ROSAT	50054.000	1.41305(12)	Kahabka & Li 1999
RXTE	50091.170	1.41308143(16)	Wojdowski et al 1998
00011	50093.048	1.4130802(13)	This paper
00011	50093.115	1.4130802(39)	This paper
00011	50093.181	1.4130786(14)	This paper
10139	50323.016	1.41361728(15)	This paper
10139	50323.349	1.4136112(52)	This paper
10139	50324.010	1.413626129(76)	This paper
10139	50325.069	1.41362903(34)	This paper
10139	50326.009	1.413627028(64)	This paper
10139	50327.268	1.4136316(18)	This paper
10139	50327.941	1.413637100(64)	This paper
10139	50328.993	1.413640077(64)	This paper
10139	50329.940	1.413637060(64)	This paper
20146-20109-20417	50411.87	1.413823(17)	This paper
20146-20109-20417	50442.90	1.413918(16)	This paper
BeppoSAX-1	50460.900	1.413971(16)	Naik & Paul et al 04

<sup>1</sup> errors indicated in the paranthesis gives the value for each pulse period in  $1\sigma$

Proposal ID or Observatory	MJD (days)	Pulse Period <sup>1</sup>	References
20146-20109-20417	50489.366	1.4140261(14)	This paper
20146-20109-20417	50504.524	1.4140567(16)	This paper
20146-20109-20417	50505.169	1.4140587(18)	This paper
BeppoSAX-2	50507.600	1.414067(8)	Naik & Paul et al 04
20146-20109-20417	50531.806	1.4141297(10)	This paper
20146-20109-20417	50535.679	1.4141399(14)	This paper
20146-20109-20417	50551.398	1.4141789(10)	This paper
20146-20109-20417	50556.346	1.414180(15)	This paper
BeppoSAX-3	50562.100	1.414199(14)	Naik & Paul, 2004
20146-20109-20417	50566.861	1.4142307(9)	This paper
20146-20109-20417	50579.511	1.414251(16)	This paper
20146-20109-20417	50583.009	1.4142586(5)	This paper
20146-20109-20417	50583.030	1.4142597(14)	This paper
ROSAT	50593.799	1.41430(2)	Kahabka & Li, 1999
20146-20109-20417	50597.960	1.414306(2)	This paper
20146-20109-20417	50598.980	1.4143059(14)	This paper
20146-20109-20417	50609.319	1.414340(5)	This paper
20146-20109-20417	50617.757	1.4143399(96)	This paper
20146-20109-20417	50617.898	1.41433(5)	This paper
20146-20109-20417	50646.787	1.414420(7)	This paper
20146-20109-20417	50675.866	1.414488(13)	This paper
20146-20109-20417	50711.833	1.41457(2)	This paper
20146-20109-20417	50738.053	1.414631(10)	This paper
20146-20109-20417	50767.442	1.414706(10)	This paper
20146-20109-20417	50795.116	1.41477(7)	This paper
30125	50850.541	1.414891(5)	This paper
30125	50883.272	1.41497(2)	This paper
ROSAT	50898.200	1.41501(2)	Kahabka & Li, 1999
30125	50910.965	1.4150(2)	This paper
30125	50949.407	1.415116(5)	This paper
30125	50949.751	1.41512(6)	This paper
30125	50950.048	1.415128(11)	This paper
30125	51007.374	1.41524(6)	This paper
30125	51007.975	1.415242(7)	This paper
30125	51060.725	1.41538(5)	This paper
30125	51060.791	1.41538(4)	This paper
30125	51061.265	1.415376(18)	This paper

<sup>1</sup> errors indicated in the paranthesis gives the value for each pulse period in  $1\sigma$

Proposal ID or Observatory	MJD (days)	Pulse Period <sup>1</sup>	References
30090-30125	51102.221	1.41548(9)	This paper
30090-30125	51106.083	1.41548(2)	This paper
30090-30125	51108.060	1.415432(18)	This paper
30090-30125	51109.781	1.41543(3)	This paper
30090-30125	51111.866	1.41544(2)	This paper
30090-30125	51113.711	1.415443(4)	This paper
30090-30125	51115.709	1.415446(6)	This paper
30090-30125	51117.607	1.415451(20)	This paper
30090-30125	51119.586	1.415455(4)	This paper
30090-30125	51121.160	1.415509(2)	This paper
30090-30125	51121.515	1.4155127(14)	This paper
30090-30125	51121.637	1.41552(11)	This paper
30090-30125	51121.724	1.41551(4)	This paper
30090-30125	51125.443	1.41552(7)	This paper
30090-30125	51127.234	1.415528(17)	This paper
30090-30125	51129.376	1.41553(10)	This paper
30090-30125	51131.300	1.41553(5)	This paper
30090-30125	51133.301	1.41555(6)	This paper
30090-30125	51151.014	1.41559(3)	This paper
30090-30125	51151.416	1.41558(3)	This paper
40064	51699.405	1.416816(9)	This paper
40064	51699.666	1.416824(9)	This paper
40064	51699.736	1.41681(3)	This paper
40064	51699.876	1.416812(16)	This paper
40064	51700.172	1.41681(6)	This paper
40064	51700.233	1.416809(22)	This paper
40064	51700.383	1.416809(20)	This paper
40064	51700.593	1.41681(9)	This paper
40064	51700.663	1.416808(47)	This paper
40064	51700.803	1.416810(14)	This paper
40064	51700.896	1.416807(57)	This paper
40064	51701.152	1.416814(45)	This paper
40064	51701.315	1.416817(3)	This paper
40064	51701.590	1.41682(13)	This paper
40064	51701.660	1.416819(43)	This paper
40064	51701.869	1.416822(33)	This paper
40064	51701.957	1.4168218(3)	This paper

<sup>1</sup> errors indicated in the paranthesis gives the value for each pulse period in  $1\sigma$

Proposal ID or Observatory	MJD (days)	Pulse Period <sup>1</sup>	References
Chandra	51833.808	1.4170032(6)	Vrtilek et al 2005
INTEGRAL	52843	1.419253(16)	McBride et al 2007
80078	52939.611	1.419470(5)	This paper
80078	52939.680	1.419472(6)	This paper
80078	52939.749	1.4194708(19)	This paper
80078	52940.527	1.4194728(50)	This paper
80078	52940.596	1.419473(34)	This paper
80078	52940.665	1.41947(3)	This paper
80078	52940.734	1.4194722(15)	This paper
80078	52940.805	1.419471(3)	This paper
80078	52940.958	1.419470(13)	This paper
80078	52941.304	1.419468(50)	This paper
80078	52941.373	1.419465(38)	This paper
80078	52941.442	1.419464(36)	This paper
80078	52941.511	1.419464(11)	This paper
80078	52941.813	1.419460(4)	This paper
80078	52942.289	1.419462(2)	This paper
80078	52942.565	1.419466(33)	This paper
80078	52942.652	1.419469(76)	This paper
80078	52942.825	1.41947(28)	This paper
80078	52942.891	1.41947(35)	This paper
80078	52943.688	1.419481(6)	This paper
80078	52981.226	1.4195(4)	This paper
80078	52981.527	1.41955(13)	This paper
80078	52982.064	1.419578(10)	This paper
80078	52983.496	1.41958(3)	This paper
80078	52984.033	1.419572(6)	This paper
80078	52984.360	1.419570(45)	This paper
80078	52984.480	1.419567(36)	This paper
80078	52984.687	1.419566(12)	This paper
80078	52984.890	1.419566(16)	This paper
80078	52985.326	1.419571(7)	This paper
80078	52986.311	1.419586(25)	This paper
80078	52987.433	1.419587(39)	This paper
80078	52987.640	1.419585(43)	This paper

<sup>1</sup> errors indicated in the paranthesis gives the value for each pulse period in  $1\sigma$

Table 4: Long Term Spin-up Rate Values of SMC X-1

Interval (MJD-MJD)	Spin-up Rate ( $10^{-11}$ Hz s $^{-1}$ )
41000-42850	3.59(48)
42950-46100	2.3718(15)
46900-47800	2.2491438(1)
48450-49200	1.9528(38)
50093-52988	2.65343816(7)

Table 5: Sample Spectral Parameters from Two Different Observations

Obs ID	10139-01-01-00	20146-06-02-00
MJD	50323.349	50442.905
nH( $10^{22}$ cm $^{-2}$ )	12.039 $\pm$ 0.748	2.214 $\pm$ 0.290
Powerlaw Index	1.184 $\pm$ 0.043	1.176 $\pm$ 0.074
$E_{cutoff}$ (keV)	13.697 $\pm$ 3.424	6.595 $\pm$ 1.649
$E_{fold}$ (keV)	11.765 $\pm$ 4.118	10.020 $\pm$ 3.507
( $\chi^2_\nu$ ) (degrees of freedom)	0.868(47)	1.055(47)
Observed flux ( $10^{-10}$ ergs cm $^{-2}$ s $^{-1}$ )(3-25 keV)	2.3866 $^{+0.0282}_{-0.102}$	20.673 $^{+0.043}_{-0.157}$
Unabsorbed flux ( $10^{-10}$ ergs cm $^{-2}$ s $^{-1}$ )(3-25 keV)	2.8281 $^{+0.002}_{-0.012}$	21.553 $^{+0.039}_{-0.078}$